

Methods for Collision-Free Arm Teleoperation in Clutter Using Constraints from 3D Sensor Data

Adam Leeper^{1,2}, Kaijen Hsiao², Matei Ciocarlie², Ioan Sucan², and Kenneth Salisbury¹

¹Stanford University, Stanford, California, USA.

²Willow Garage, Inc., Menlo Park, CA, USA.

Abstract—We introduce CAT, a constraint-aware teleoperation method that can track continuously updating 6-DOF end-effector goals while avoiding environment collisions, self-collisions, and joint limits. Our method uses sequential quadratic programming to generate motion trajectories that obey kinematic constraints while attempting to reduce the distance to the goal with each step. Environment models are created and updated at run-time using a commodity depth camera. We compare our method to three additional teleoperation strategies, based on global motion planning, inverse kinematics, and Jacobian-transpose control. Our analysis, using a real robot in a variety of scenes, highlights the strengths of each method, and shows that the CAT method we introduce performs well over a wide range of scenarios.

I. INTRODUCTION

Deployment of mobile manipulators in human settings could be accelerated by including human-in-the-loop system components. Teleoperation could be used for the more-difficult components of a task, leaving the rest to autonomy, or as a fallback option if autonomy fails. However, teleoperation can be tedious and difficult. Highly-articulated arms often have non-anthropomorphic configurations, non-intuitive workspaces and joint limit constraints. Controlling such arms is made more difficult when trying to also avoid collisions with objects in cluttered human environments.

One way to address this problem is to create tools that leverage autonomous capabilities even during operator-guided motions. In this paper, we explore how to use control and planning methods to allow an operator to command an end-effector pose without worrying about kinematics or collision avoidance, leaving those tasks to the robot. Along the way we introduce CAT, a locally-optimal trajectory generation strategy based on sequential quadratic programming.

A. Problem Description and Goals

Our problem set-up includes a robot equipped with a dexterous (7-DOF) arm. A remote operator controls the robot's arm by moving a Cartesian end-effector goal pose, and the robot continuously tries to track the current goal. Focusing on applicability to complex tasks in unstructured and cluttered environments, the problem is set up as follows:

- The goal is specified as a 6-DOF gripper pose, allowing for general end-effector movement while not requiring the operator to reason about the kinematics of the arm.
- The operator can continuously update the goal, without first waiting for the robot to achieve previous goals.

- The robot does not have a pre-constructed map of obstacles in the environment, but instead maintains a continuously-updating model of obstacles using a live stream of data from its sensors (e.g. Kinect depth camera).

Our goal in this paper is to compare methods for tracking the end-effector goal specified as above, while enabling the user to focus on task completion rather than joint-level constraints. At each time step, the chosen arm control method takes as input the current configuration of the arm as well as the current goal pose, and outputs joint torques. In designing our arm control methods, we aspire to the following goals:

- Tracking: the end-effector should track the goal pose. When the goal is unachievable (as defined by the constraints below), the end-effector should follow as closely as possible.¹
- Collision avoidance: the robot should avoid undesired collisions anywhere on the arm.
- Joint limit avoidance: the arm configuration should avoid having joints close to or against their limits, to increase manipulability and make future goals easier to achieve.

B. Contributions

This work is the first, to the best of our knowledge, to examine the problem of tracking a continuously-updating 6-DOF end-effector pose while avoiding contact with a volumetric model generated in real-time from visual sensing.

We propose a constraint-aware teleoperation (CAT) controller based on sequential quadratic programming which enables us to meet the tracking and obstacle avoidance goals set forth above. In order to analyze the performance of CAT, we implemented three other teleoperation strategies for comparison, based on extensions to established arm-motion methods:

- Joint-space global motion planning (MP), using sampling-based planning to continuously replan as the goal changes.
- Collision-aware inverse kinematics (IK), combining IK for the goal pose, joint-space interpolation, and collision detection to find a collision-free trajectory.
- Jacobian transpose torque control (JT), with no additional constraint or collision avoidance capabilities.

In our experimental section we quantify and compare the behavior of each approach over a common set of experiments.

¹The exact definition of “closeness” may be task dependent; this paper assumes end-effector Cartesian pose error is the dominant factor.

II. RELATED WORK

Our work draws from many areas of research in telerobotics, including control, haptics, and motion planning.

Dragan and Srinivasa [6] formalized the “do what I mean” problem in teleoperation by defining an *arbitration* or policy-blending component of the control loop. The CAT method (and each alternative) can be viewed as an arbitration strategy where the user provides input, the robot “predicts” geometric constraints from sensor data, and CAT creates a motion that attempts to satisfy both. Unlike [6], however, we are concerned with general arm motion rather than specific task prediction.

Control methods in telerobotics typically compute torques that “pull” a system toward one or more goals while pushing it away from obstacles. Potential fields [12] are one such method; circular fields [7] are better at avoiding local minima. Sentis and Khatib [28] outline a method for hierarchical control of task goals and constraints in which each goal is achieved as closely as possible using artificial potential fields in the nullspace of all higher-priority goals. Passenberg et al. [23] provides an excellent summary of several methods for improving bilateral teleoperation by adapting controllers to the environment, operator, or task.

We draw some inspiration from haptic rendering methods; we use a kinematic “proxy” for the robot state, and the pose error is expressed through a virtual-coupling [4]. (Our system can render the virtual coupling forces to the operator through a haptic device, but this paper does not explore that aspect.) Since we use a proxy and a sensor-based environment model to compute motions, our system is a type of model-mediated teleoperation [20]. In this context our motion constraints are also a form of forbidden-region virtual fixtures [1] created in real-time from sensor point clouds. Mitra and Niemeyer [19] used constraints from model-based geometric collision detection to avoid self-collisions and generate haptic force feedback while teleoperating two 6-DOF arms, but they did not do any environmental collision avoidance.

Randomized motion planning in arm configuration space is very popular in autonomous robot systems [5], but it has only recently reached the speed necessary for responsive performance with continuously updating goals. Hauser [9] tested a motion planning approach for teleoperation of 3-DOF tasks that is very similar to the MP method we use; however, our method uses 6-DOF end-effector goal poses, and is implemented and tested on a real robot using live sensor data for collision avoidance. Knepper et al. [13] proposed a hierarchical planning method to greatly improve responsiveness, using a rough global planner to guide a local planner.

Several recent studies have used sequential quadratic programming methods for fast generation of robot motion plans, though none have used these methods in teleoperation of a real robot or with an emphasis on real-time collision avoidance. Posa and Tedrake [25] focused on the problem of planning through rigid-body contact, applied to generation of walking trajectories; Werner et al. [29] similarly optimized

walking motions. Lampariello et al. [15] created optimal trajectories for catching a ball in real-time, demonstrated in simulation. Pham and Nakamura [24] demonstrated trajectory deformation and motion stitching in response to new motion goals. Finally, Schulman et al. [27] showed robust motion-planning using a similar formulation to ours, but they (and the other strategies above) spend time obtaining global trajectories because they are designed for use in autonomous robotic systems. In our context, we assume the human operator fills the role of a “global planner,” so CAT creates local plans at a rate one order of magnitude higher than those in [27].

Most similar to our work, Jain et al. [11] used sequential quadratic programming to enforce joint limit and contact constraints while trying to reach a 6-DOF target. The contact constraints in their work are generated using force sensors and are intended to limit (but not eliminate) contact with obstacles. This strategy is complementary to ours; visual sensors alone cannot predict collisions with invisible or occluded obstacles, while force sensors alone cannot avoid contact with fragile or light obstacles for which even minor contact can be disastrous. Using a full collision map generated by visual depth sensing allows the CAT method to compute a multi-step trajectory (Sec. IV-D), producing smoother and faster motion. Detecting contact points only through force sensing means that the robot has no geometric model of obstacles before hitting them and thus cannot predict contacts in advance.

III. TELEOPERATION SYSTEM OVERVIEW

We begin with an overview of our system in order to provide context for the teleoperation strategies described later.

The input command is a 6-DOF end-effector pose read from the operator at 30 Hz. In our implementation, the pose can be commanded through mouse interaction with on-screen controls, or through a 6-DOF Razer Hydra input device.

Each teleoperation strategy is responsible for processing this input pose at every time step and sending a command to the appropriate low-level controller. Fig. 1 shows the system block diagram for three of our strategies: CAT (Sec. IV), MP (Sec. V-B), and IK (Sec. V-A). These three methods all generate a trajectory of joint configurations which is passed to a low-level joint trajectory follower. Quintic splines between joint trajectory points are computed and passed to a standard joint impedance controller. By contrast, the JT method (Sec. V-C) simply passes the goal pose directly to a low-level Jacobian-transpose controller not shown in the diagram. After processing a goal command, each strategy restarts using the most recent goal pose. Section IV-D describes how we ensure continuity of trajectories while the robot arm is in motion.

We assume that the robot has joint encoders for measuring its own kinematic configuration, and one or more sensors for perceiving the environment. Our implementation uses a commodity depth camera to build a continuously-updating volumetric representation of the world, which is used for

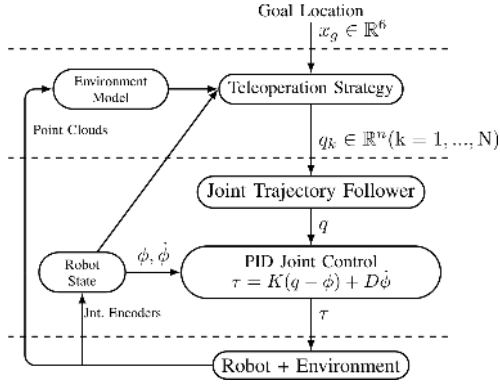


Fig. 1. Block diagram showing the hierarchical control structure for the CAT, MP, and IK methods. The number of joints is denoted by n , and N is the number of trajectory points.

predicting (and avoiding) collisions in the CAT, MP, and IK strategies as described in section IV-B.

IV. CONSTRAINT-AWARE TELEOPERATION STRATEGY

The first method we describe is the Constraint-Aware Teleoperation (CAT) controller, one of the main contributions of this study. In general terms, CAT creates joint trajectories by computing incremental joint position changes that reduce the value of a cost function while simultaneously obeying a set of constraints. It is designed to be used in a local fashion, quickly computing small steps away from a known joint configuration, but not expected to be globally optimal. We argue that in the domain of teleoperation it is valuable to have an option that combines responsiveness and constraint-awareness.

We formulate the problem as an instance of convex optimization, namely a quadratic program (QP) with linear inequality constraints that operates on a (time-varying) linearized model of the robotic system. The solution to the QP represents a small incremental change to the state of the system. The QP is reformulated after each step due to the nonlinear kinematics and because each new kinematic configuration may result in new constraints due to predicted contact with the environment. We note that our problem is formally an instance of linear model predictive control [21] (MPC) where each step has a time horizon of length one.

We note that each iteration of the QP solves for a single joint step, but in each command period the QP is run many times² to create a continuous trajectory (see section IV-D).

A. Quadratic Program Formulation

We wish to compute joint deltas, Δq , that move us closer to a goal expressed as a quadratic objective function. In our QP, the optimization variables are $\Delta q \in \mathbb{R}^n$, where n is the number of joints, and the objective is a sum of quadratic functions of the optimization variables. In particular, our **QP objective** is composed of three parts:

²We use CVXGEN, a tool that generates highly-optimized, problem-specific C-code (www.cvxgen.com) [18]. This allows each QP step to be solved orders of magnitude faster (around 200-400 μ s) than if using a generic solver, allowing us to take small steps (for fine-grained constraint checking) while computing a longer trajectory in each period.

1) *Move toward a goal pose:* For a desired Cartesian goal pose, $x_d \in \mathbb{R}^6$, we compute the necessary pose change, Δx_d , from the proxy end-effector pose. Since our linear system model is only valid for small displacements the error is clipped to a maximum distance and angle of rotation when computing Δx_d . With the end-effector Jacobian $J \in \mathbb{R}^{6 \times n}$ and a weighting matrix $W_x \in \mathbb{R}^{6 \times 6}$, the objective term is:

$$(\Delta x_d - J \Delta q)^T W_x (\Delta x_d - J \Delta q). \quad (1)$$

2) *Discourage large joint changes:* This term encourages the optimized variables to stay small. Even for a small Cartesian movement, certain configurations can result in solutions with large joint displacements, which is an artifact of the linearized system. Defining a diagonal weighting matrix $W_{\Delta q} \in \mathbb{R}^{n \times n}$, the objective term is

$$\Delta q^T W_{\Delta q} \Delta q. \quad (2)$$

3) *Reach a given joint posture:* This term encourages the joints to move toward a desired vector of joint positions, q_d . A “passive” way to use this term is to set $q_d = (q_{max} + q_{min})/2$, which has the effect of biasing each joint toward the center of its workspace and away from joint limits. Alternatively, q_d can be actively commanded; for example, if q_d is set to the value of an IK solution and the other objective terms are given zero weight, this term basically turns the entire CAT controller into an IK controller that obeys constraints. Defining the weighting matrix as $W_q \in \mathbb{R}^{n \times n}$, the objective term is:

$$((q + \Delta q) - q_d)^T W_q ((q + \Delta q) - q_d) \quad (3)$$

The **QP constraints** are defined as follows:

1) *Obey joint limits:* Simply put, the incremental joint change may not push any joint past its position limits.

$$q_{min} \leq (q + \Delta q) \leq q_{max} \quad (4)$$

2) *Do not move in the direction of contact:* After each step, the collision detector checks for contact with the environment model, providing a point, $c_i \in \mathbb{R}^3$, and normal, $n_i \in \mathbb{R}^3$, for each contact. On the subsequent step this contact set is used to constrain the change in position of each contact point. The velocity Jacobian is computed for each contact point and is denoted $J_{c_i} \in \mathbb{R}^{3 \times n}$. We assume that motion perpendicular to the contact normal is acceptable, but the point of contact may not move further into collision:

$$n_i^T (J_{c_i} \Delta q) \geq 0. \quad (5)$$

Additional objective terms or constraints are certainly possible. For example, while the contact constraints used in this paper can be viewed as an example of forbidden-region virtual fixtures [1], terms could be added to the objective to help a user follow a particular path or track a moving object.



Fig. 2. Left: a teleoperated robot performing a manipulation task in a cluttered environment. Right: the scene as seen by the operator, with visual controls (colored rings and arrows) used for specifying end-effector pose goals, and the robot's collision map temporarily overlaid for visualization.

B. Collision Detection

Collision detection is a key component of the CAT, MP, and IK strategies. Our system uses a commodity depth camera to build a continuously-updating volumetric representation of the world. Specifically, we use the Flexible Collision Library (FCL) [22] to perform collision checks with an octree representation of the environment maintained using the Octomap library [10]. An example of a real-world scene and the corresponding Octomap is shown in Fig. 2. We note that the robot's body is filtered out of the point cloud data before updating the Octomap; filtering is reliant on reasonably good forward-kinematics and a "padding" parameter around the robot links.

Since the Octomap provides a quantized world model, normals provided by the mesh-octree collision detection algorithm are typically aligned with the faces of the underlying octree cells. To help smooth the normals, (and hence, the constraints), our implementation uses a normal-refinement step, illustrated in Fig. IV-C. Each contact point is used to query the center-points of nearby occupied octree cells. Those points are assigned compactly-supported radial basis functions that are used to estimate an implicit field at the contact point, yielding a more accurate normal. This is a direct application of the algorithm described in Leeper et al. [17], with the metaball radius set to 1.5 times the octree cell size. We note that collision detection is by *far* the most expensive part of the trajectory computation process, taking on the order of 1 ms per check in our implementation.

C. Step Validation

In the CAT controller, collisions are computed after each QP step. The updated kinematic state is used to find the contact points and normals between the robot model and the environment model. Steps that have taken the robot into a colliding state can be accepted or rejected depending on the tolerance for predicted collisions. The contact information is used to formulate the constraints on the next QP step, which will prevent further motion into the contact constraint. We note that cases of desired contact, such as between the gripper and the environment, can be handled by disabling collision checking for links or objects that should not be constrained.

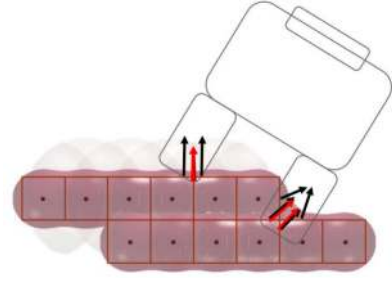


Fig. 3. Contact normals reported for contact with occupied cells in the Octomap (orange boxes) are re-computed against an implicit metaball surface representation (wavy red surroundings). This helps to mitigate the "stair-step" nature of the Octomap and provides better constraints.

D. Generating Suitable Motion Trajectories

The CAT, MP and IK methods each generate joint-space trajectories which are executed on the robot by a low-level 1kHz joint impedance controller. In general, the following elements complicate the relationship between responsiveness, speed, and safety in our teleoperation strategies:

1) *Velocity Limits*: The trajectory of joint motions generated via CAT (and the IK method) is checked for collisions. The number of steps is limited by computation time in each command period, so the robot has a finite horizon in which it can predict constraints. Hence, the robot must limit joint velocities such that each joint can come to a complete stop at the end of any given trajectory. Otherwise, this could lead to an inevitable collision state, where the robot is unable to stop in time to avoid obstacles that appear suddenly.

Since longer computed trajectories will result in higher allowable movement speed, we run the CAT and IK methods at 30 Hz (which is the update rate of the user command input) and compute as many steps as possible in the allotted time (approximately 15-20 in our implementation), as opposed to sending a single trajectory point at a time at a much faster rate (about 400 Hz on current hardware). This is a major difference from the MPC used in [11], which must compute a single point at a time and move slowly since the collision detection comes from force-contact sensors and cannot be predicted.

2) *Continuity*: The trajectory that was most recently sent to the joint trajectory follower will be partially executed by the time a new trajectory result is available. Hence, it is necessary to ensure continuity of commanded joint positions and velocities when splicing in the new trajectory.

Each strategy is responsible for returning a result before a time limit, t_f , at the end of each command period. The starting state, q , for the computation is picked to be the first point in the previous trajectory that was scheduled to be executed after t_f . Assuming the trajectory is computed in time, it can be spliced into the execution queue.

If a trajectory is not computed in time for any reason, the result must be discarded altogether. To prevent repeated failure due to insufficient time, we use an adaptive command period (similar to [8]), allowing more time if the previous computation failed and less time if there was time to spare.

We note that this adaptive timing is most important for the MP strategy, since the incremental nature of CAT and IK means they can work within a given time limit.

V. ALTERNATIVE METHODS

We implemented three established approaches to arm teleoperation for comparison to our CAT method. Each method represents a different technique for approaching the problem stated above, each with advantages and disadvantages, depending on the situation.

A. Collision-Aware Inverse Kinematics (IK)

In each command period (at 30 Hz), for the current end-effector goal pose, we look for a set of collision-free joint angles that achieve the goal. For a robot arm with 7+ degrees of freedom, there is an infinite set of joint angles that place the end-effector at any reachable goal. The IK solver for the 7-DOF arm on the PR2 robot searches over the space of redundant joint angles by iterating over the range of possible values for one joint and using an analytical IK solver to rapidly compute the other six, checking the resulting configuration for collisions until a collision-free solution is found. The search is formulated to avoid large changes in joint values when possible, to avoid unpredictable arm motions due to small changes in commanded end-effector pose. If the IK search is successful, we create a trajectory to the goal using linear interpolation in joint-space. A collision check is performed for each step in the interpolation, ensuring the motion will avoid collisions. If the command period will be exceeded by checking the entire trajectory, a partial trajectory is used (section IV-D), and the computation picks up again during the next command period.

B. Motion Planning (MP)

Motion planning can be used to compute continuous, collision-free joint space trajectories that connect start and goal configurations of a robot [16]. For higher dimensional systems (e.g., robot arms), sampling-based planning algorithms are starting to approach the computational efficiency and responsiveness needed for arm teleoperation. Our MP method uses RRT-Connect [14], a bi-directional sampling-based planner implemented in OMPL [5], to compute a trajectory to the most recent goal configuration (which is found using collision-free inverse kinematics as described above). Recent benchmarks [3] show that RRT-Connect works well in typical manipulation settings. We found that other bi-directional planners (e.g., SBL [26]) produce similar results, while single-tree planners significantly increase planning times. Due to their randomization, sampling-based planners typically produce jerky, unpredictable paths. To alleviate this problem we also run a standard randomized path shortening algorithm on every computed motion plan.

Motion planning has the advantage of operating in the global configuration space, and is able to find paths that take locally error-increasing steps in order to escape local minima. The downside is the additional computation time needed; the MP method was run at a nominal rate of 4 Hz

(with adaptive timing as needed). Unlike previous work using motion planning in a teleoperation task [9], our analysis is applied to a real robot, uses real sensor data for collision avoidance, and tracks goal poses in all 6 DOF of translation and rotation.

C. Jacobian-transpose Control (JT)

This method tracks the Cartesian goal using a standard torque control law of the form

$$\tau_p = J^T \mathbf{f}, \quad (6)$$

where \mathbf{f} is a wrench computed from the error between the actual gripper pose and the goal pose at 1 kHz. New goal poses are sent to the controller at 30 Hz.

Since 7-DOF arms have one redundant degree of freedom after constraining the end-effector pose, we additionally bias the arm towards a desired neutral posture (which could be robot- or task-dependent, or specified by the operator) by adding nullspace joint torques (τ_n) to the controller:

$$\tau_n = \mathbf{k} * (I - J^\dagger J) * \mathbf{q}_e \quad (7)$$

where \mathbf{q}_e are the joint differences between the current and desired posture, J^\dagger is the Jacobian pseudo-inverse, and \mathbf{k} is a vector of joint gains. The final torques sent to the joints are a combination of the pose-tracking torques and the nullspace posture torques:

$$\tau = \tau_p + \tau_n \quad (8)$$

In addition to goals such as posture control, Jacobian-transpose controllers can explicitly be made somewhat collision-aware by layering goals, each in the nullspace of the last. However, avoiding unwanted collisions by making it a secondary goal in the nullspace of a pose goal does not prevent collisions from happening if the pose goal cannot be reached without colliding. Conversely, making a pose goal a secondary goal in the nullspace of a goal that only avoids collisions can prevent the end effector from reaching the pose goal when potential collisions are nearby, even if the arm could be moved into a configuration that accomplishes both goals together. Chiaverini [2] explores some of these issues in task-priority and redundancy resolution.

Even in non-collision-aware form, a Jacobian-transpose control law is often used for teleoperation when trying to control the forces exerted at an end effector. Adding an impedance matrix allows the controller to exert different maximum forces at the end effector in various task-space directions, for tasks such as wiping a surface or turning a crank. For example, if the contact normal for a surface in collision with the end-effector is known, it is possible to change the impedance matrix to better avoid pushing with high force into the surface, while sliding along it with high stiffness in a tangential direction. For our experiments, we do not change the impedance matrix according to contact normal, but we do limit the overall magnitude of the desired Cartesian wrench.

Unlike our Collision-Aware IK method, Jacobian-transpose controllers are good at getting close to unreachable

goals or goals in collision, since a Cartesian pose goal does not need to be feasible in order to result in valid incremental joint torques according to the Jacobian-transpose control law.

VI. EXPERIMENTAL RESULTS

We implemented, tested and compared all the teleoperation methods described above on a variety of scenes and trajectories. The hardware consisted of a PR2 robot, equipped with a 7-DOF arm. For environment sensing we used a Kinect sensor mounted on the robot's head.

For each scene, we used one of the two input devices described in Sec. III (mouse and Razer Hydra) to record a trajectory of end-effector goals over time. Starting from the same initial robot pose, the recorded goal trajectory was then played back for each of our teleoperation methods, and the resultant arm motion was recorded. In addition, we used a 6 DOF force/torque sensor mounted in the wrist to record end-effector forces from contacts with the environment. We note that all collision-aware methods discussed in this paper use only the data from the Kinect to build obstacle models. Furthermore, even though all the collision-aware methods reason about collisions anywhere on the arm, our hardware only permitted us to record collision forces and torques on the end-effector.

The first scene (fig. 4a) did not contain any obstacles. While the focus of our methods is efficient operation in cluttered settings, numerous tasks will contain at least parts of the trajectories where no obstacles play a role, and good tracking in these region is important for overall efficiency. We present two cases: a *step input* where the goal pose is directly set to the desired final pose of the gripper; and a *continuous input* where the goal is moved from the starting location of the gripper to its desired final pose over the course of approximately 1.5s. We believe the second case to be more representative of real-life teleoperation, where the operator continuously updates the goal and moves it towards the desired location.

We notice that all four methods track the desired pose. We focus in more detail on two metrics: response time (time after a new goal is specified until the arm starts to move) and total time (needed to reach the goal). As expected, JT achieves the lowest times for both metrics, while MP is the slowest. In the step input case, CAT shows lower response time but higher total time than MP; in the continuous input case, it achieves lower times on both metrics, ranking immediately behind JT.

Fig. 4b looks at a case where the direct path to the specified goal is blocked by obstacles (in this case, boards clamped to the table). As seen in the tracking results, the JT method gets physically stuck on the boards due to friction, and the IK method detects the impending collision along the path and stops; neither method reaches the final goal. MP is able to plan a path around the obstacles, though it has some trouble following the continuously moving goal as it passes through infeasible locations. CAT performs the best in this scenario as it is able to follow the goal quite closely while “sliding” up and over the virtual constraints without actually touching the boards (as shown in the force data).

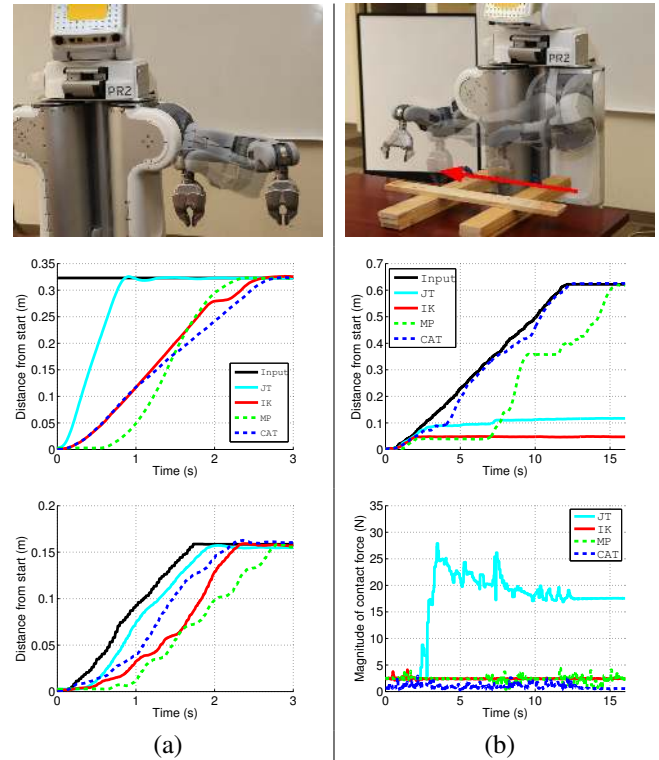


Fig. 4. (a) Response to free-space motion between a starting robot pose (transparent) and the goal end-effector pose (opaque). The top plot shows tracking results for a step input, showing the distance from the starting pose over time, for both the goal pose and the end-effector pose achieved by each teleoperation method. The bottom plot shows results for a continuous input. (b) Motion across a set of rigid boards 9 cm wide, 6 cm high, and 24 cm apart, in response to a *continuous input* translation.

We note that in the scene of Fig. 4b the obstacles do not create a local minimum. However, in a case where the straight path to the goal is perpendicular to the obstacle surface (Fig. 5a), local methods such as JT and CAT are unable to escape. MP is able to plan a path that temporarily increases tracking error in order to eventually reach the goal.

Fig. 5b demonstrates how joint limit constraints affect the presented methods. In this common scenario, the operator wishes to move the gripper from pointing down to pointing up. Due to the wrist pitch joint limit and the resulting singularity when the wrist is straight, the “correct” way to do this is to rotate the forearm. However, many operators who are unfamiliar with the kinematic limits, the effect of friction in the mechanism, or the implications of singularity avoidance instead try to pitch the wrist up through its joint limit. To investigate this source of frustration, the goal pose was rotated through this wrist pitch limit using a continuous input. By tracking the input directly, JT gets stuck against the wrist pitch joint limit with the gripper in a horizontal pose. In contrast, CAT, MP, and IK are able to keep the arm away from joint limits and reach the goal (the final pose as achieved by MP is shown in the image).

Fig. 5c shows the case where part of the goal trajectory is outside the robot’s workspace. Here we notice that MP and IK simply stop tracking while the goal is unreachable (from 4 seconds to approximately 8.5 seconds into the trajectory). In contrast, JT and CAT track the goal along the edge of the

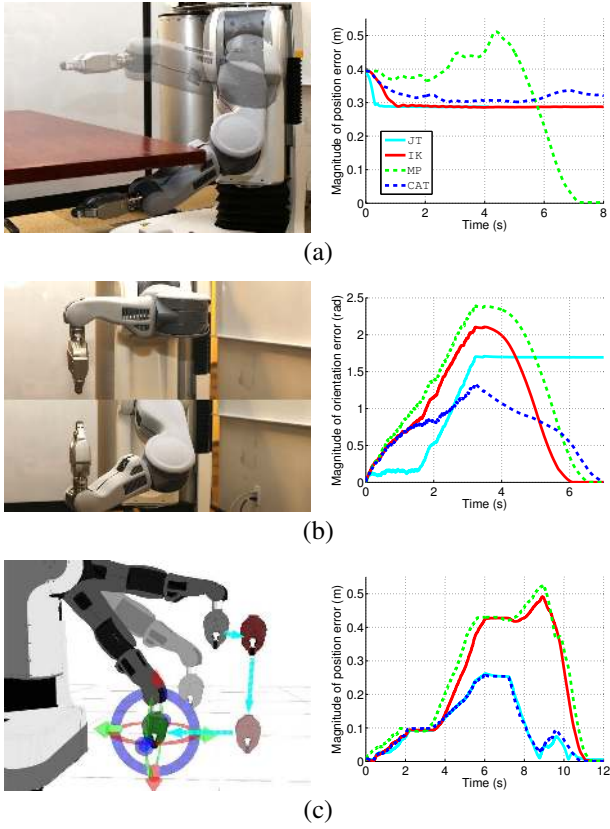


Fig. 5. Additional constrained teleoperation examples. a) Collision constraint perpendicular to straight line motion to goal. b) Straight path to goal hits joint limit (starting with gripper pointing down and ending with gripper pointing up). c) Part of the goal trajectory is outside the robot's workspace. In this case, end-effector goals outside the workspace are shown as disembodied grippers; closest reachable gripper pose for the goal in the bottom right is shown as a transparent robot posture. (Plot colors are consistent across all figures.)

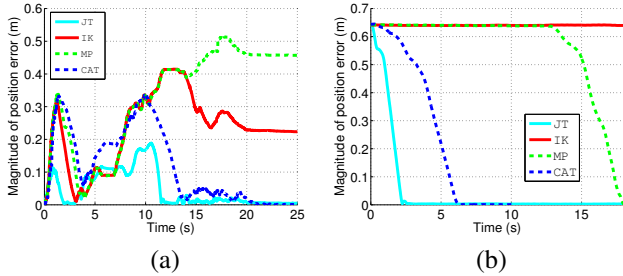


Fig. 6. a) Tracking results for reaching into a shelf with a collision-free goal trajectory. b) Results for exiting the shelf with a colliding goal trajectory.

workspace. Some single-tree motion planners [30] can move toward infeasible goals; while we selected a bi-directional planner for improved performance in most cases, a logical extension would be to run multiple planners in these cases.

To show off more general, overall behavior in a typical cluttered scene, Fig. 6 plots tracking results for reaching into and retreating out of the cluttered shelf shown in Fig. 2. The goal trajectory for the reach in was demonstrated with a Razer Hydra, with the operator being careful to select goal poses that were not colliding. Tracking error is shown in Fig. 6a. In this case, JT performs best because the goal poses happen to be collision-free. CAT follows close behind, with

the larger tracking error due to joint limit avoidance. IK gets stuck because of momentarily infeasible goals. MP follows the initial part of the trajectory, then stops, and eventually moves to the goal (the plot is truncated to better show the behavior of the other methods). Fig. 6b shows results for the retreat, in which the goal trajectory collides with the shelf. JT again gets there fastest, but hits the shelf with high force (peak of 35 N) on the way. CAT follows close behind without hitting the shelf, IK gets stuck, and MP eventually gets there.

VII. DISCUSSION AND CONCLUSIONS

In this paper, we focused on the problem of assisted teleoperation in unstructured environments based on visual sensing. We introduced CAT, a constraint-aware teleoperation controller based on sequential quadratic programming, which continuously attempts to reduce tracking error while taking into account constraints such as collisions or joint limits.

Manipulation in cluttered environments is by nature a highly-constrained task. In our experiments, we used a real robot and real sensor data collected during task execution to explore a number of these constraints. Our analysis included the CAT controller, as well as three additional methods: global motion planning with a continuously-updating goal pose (MP), collision-aware inverse kinematics with joint-space interpolation (IK), and Jacobian-transpose control (JT).

Our results show that each of the teleoperation methods has desirable characteristics in some situations. The JT approach is the most responsive and fastest to reach the goal in less-constrained settings, though our implementation lacks collision avoidance capabilities. (We note that, in this study, we treated all collisions as undesirable. Assuming that the robot can differentiate between undesired and desired contact, a teleoperation controller would benefit from the additional ability to regulate desired contact.) The IK approach is also very responsive in less-constrained settings, avoids colliding with itself and with the environment, and is better than JT at dealing with joint limit constraints. However, it easily gets stuck when obstacles are in the way or goals are infeasible. Since the MP method is based on global motion planning, it is the only one that will reach the goal when the others get stuck in local minima. However, it is also the least responsive of those tested, and current implementations also lack the ability to provide a “best effort” approach in cases where the goal pose is unreachable.

Based on the presented results, we believe that the CAT controller provides the best balance in terms of our stated goals: it can track constrained end-effector goal poses with a fast response, including providing “best effort” approaches to infeasible goals, avoid undesired collisions with itself and with the environment, and deal with joint limit constraints. With an operator in the loop to provide high-level motions that can take the robot around major obstacles that would cause the CAT controller to get stuck in local minima, we believe that the CAT controller is the overall winner in most situations.

However, our results also suggest that complete manipulation tasks could benefit from the strengths of each of these methods in different situations. An interesting approach for future studies would be to investigate efficient methods for combining or switching controllers based on context. However, asking the operator to actively select situationally-appropriate teleoperation methods requires a higher level of expertise and introduces delay during a task.

REFERENCES

- [1] J. Abbott, P. Marayong, and A. Okamura. Haptic virtual fixtures for robot-assisted manipulation. *Robotics Research*, pages 49–64, 2007.
- [2] S. Chiaverini. Singularity-robust task-priority redundancy resolution for real-time kinematic control of robot manipulators. *IEEE Transactions on Robotics and Automation*, 13(3):398–410, June 1997. ISSN 1042296X. doi: 10.1109/70.585902. URL <http://ieeexplore.ieee.org/lpdocs/epic03/wrapper.htm?arnumber=585902>.
- [3] B. Cohen, I. Şucan, and S. Chitta. A generic infrastructure for benchmarking motion planners. In *IROS*, 2012.
- [4] J.E. Colgate, M.C. Stanley, and J.M. Brown. Issues in the haptic display of tool use. In *IROS*, 1995.
- [5] I. Şucan, M. Moll, and L. Kavraki. The Open Motion Planning Library. *IEEE Robotics & Automation Magazine*, 19(4):72–82, December 2012.
- [6] Anca D Dragan and Siddhartha S Srinivasa. Formalizing Assistive Teleoperation. In *RSS*, 2012.
- [7] S. Haddadin, S. Belder, and A. Albu-Schäffer. Dynamic motion planning for robots in partially unknown environments. In *IFAC*, 2011.
- [8] Kris Hauser. On responsiveness, safety, and completeness in real-time motion planning. *Autonomous Robots*, 32(1):35–48, September 2011.
- [9] Kris Hauser. Recognition, Prediction, and Planning for Assisted Teleoperation of Freeform Tasks. In *RSS*, 2012.
- [10] Armin Hornung, Kai M. Wurm, Maren Bennewitz, Cyrill Stachniss, and Wolfram Burgard. OctoMap: An Efficient Probabilistic 3D Mapping Framework Based on Octrees. *Autonomous Robots*, 2013.
- [11] A. Jain, M. D. Killpack, A. Edsinger, and C. C. Kemp. Reaching in clutter with whole-arm tactile sensing. *IJRR*, 32(4):458–482, March 2013. ISSN 0278-3649.
- [12] O. Khatib. Real-Time Obstacle Avoidance for Manipulators and Mobile Robots. *IJRR*, 5(1):90–98, March 1986.
- [13] R. Knepper, S. Srinivasa, and M. Mason. Hierarchical planning architectures for mobile manipulation tasks in indoor environments. In *ICRA*, 2010.
- [14] J. Kuffner and S. LaValle. RRT-connect: An efficient approach to single-query path planning. In *ICRA*, 2000.
- [15] Roberto Lampariello, Duy Nguyen-Tuong, Claudio Castellini, Gerd Hirzinger, and Jan Peters. Trajectory planning for optimal robot catching in real-time. In *ICRA*, 2011.
- [16] S. M. LaValle. *Planning Algorithms*. Cambridge University Press, 2006.
- [17] A. Leeper, S. Chan, and K. Salisbury. Point clouds can be represented as implicit surfaces for constraint-based haptic rendering. In *ICRA*, 2012.
- [18] J. Mattingley and S. Boyd. CVXGEN: a code generator for embedded convex optimization. *Optimization and Engineering*, 13:1–27, 2012.
- [19] P. Mitra and G. Niemeyer. Haptic Simulation of Manipulator Collisions Using Dynamic Proxies. *Presence: Teleoperators and Virtual Environments*, 16, 2007.
- [20] P. Mitra and G. Niemeyer. Model-mediated telemanipulation. *IJRR*, 27(2):253–262, 2008.
- [21] M. Morari and J. H Lee. Model predictive control: past, present and future. *Computers & Chemical Engineering*, 23(4):667–682, 1999.
- [22] J. Pan, S. Chitta, and D. Manocha. FCL: A general purpose library for collision and proximity queries. In *ICRA*, 2012.
- [23] C. Passenberg, A. Peer, and M. Buss. A survey of environment-, operator-, and task-adapted controllers for teleoperation systems. *Mechatronics*, 20(7), 2010.
- [24] QC Pham and Yoshihiko Nakamura. Affine trajectory deformation for redundant manipulators. In *Robotics: Science and Systems*, 2012.
- [25] Michael Posa and Russ Tedrake. Direct Trajectory Optimization of Rigid Body Dynamical Systems through Contact. *Algorithmic Foundations of Robotics X*, 86: 527–542, 2013.
- [26] G. Sánchez and J. Latombe. A single-query bi-directional probabilistic roadmap planner with lazy collision checking. *IJRR*, 6:403–417, 2003.
- [27] John Schulman, Alex Lee, Ibrahim Awwal, Henry Bradlow, and Pieter Abbeel. Finding Locally Optimal, Collision-Free Trajectories with Sequential Convex Optimization. In *RSS*, 2013.
- [28] L. Sentis and O. Khatib. Synthesis of whole-body behaviors through hierarchical control of behavioral primitives. *Intl. J. of Humanoid Robotics*, 2(04):505–518, 2005.
- [29] Alexander Werner, Roberto Lampariello, and Christian Ott. Optimization-based generation and experimental validation of optimal walking trajectories for biped robots. In *IROS*, October 2012.
- [30] E. You and K. Hauser. Assisted Teleoperation Strategies for Aggressively Controlling a Robot Arm with 2D Input. In *RSS*, 2011.